

# Magnetolectric spectroscopy of electronic transitions in the antiferromagnet Cr<sub>2</sub>O<sub>3</sub>

B. B. Krichevstov, V. V. Pavlov, R. V. Pisarev, and V. N. Gridnev

*A. F. Ioffe Physicotechnical Institute, Russian Academy of Sciences, 194021 St. Petersburg, Russia*

(Submitted 9 April 1996)

Zh. Éksp. Teor. Fiz. **110**, 1505–1516 (October 1996)

A new type of optical spectroscopy, which makes it possible to investigate the electronic spectra of crystals without an inversion center that have macroscopically broken time-reversal symmetry and do not have a magnetic moment is proposed and implemented experimentally.

The nonreciprocal rotation of the polarization plane and the ellipticity of light reflected from the magnetolectric antiferromagnet Cr<sub>2</sub>O<sub>3</sub> in the spectral range from 1.5 to 2.5 eV, which includes <sup>4</sup>A<sub>2</sub>→<sup>2</sup>E, <sup>2</sup>T<sub>1</sub>, <sup>4</sup>T<sub>2</sub>, <sup>2</sup>T<sub>2</sub> transitions, are measured. An analysis of the spectra provides new information on the symmetry of the excited states and shows that the interpretations of the excitonic part of the spectrum in the literature are not completely consistent with the data obtained. © 1996 American Institute of Physics. [S1063-7761(96)02610-8]

## 1. INTRODUCTION

It is generally known that symmetry breaking with respect to the space-inversion operation ( $\bar{1}$ ) leads to the appearance of several optical phenomena that are forbidden in centrosymmetric media. Optical activity is the most widely known example of such phenomena.<sup>1</sup> From the standpoint of microscopic theory, space-inversion symmetry breaking results in the simultaneous appearance of nonzero matrix elements of operators between the same pairs of states  $|n\rangle$  and  $|\bar{k}\rangle$  of the medium that are even and odd with respect to the  $\bar{1}$  operation. For example, the matrix elements of the electric-dipole moment  $\mathbf{d}_{nk}$  and the magnetic-dipole moment  $\mathbf{m}_{nk}$  (or the electric-quadrupole moment) make the contributions  $g_{ij}^{(nk)}$  to the second-rank axial tensor  $g_{ij}$ , which describes the rotation of the polarization plane of light propagating in the medium:

$$g_{ij}^{(nk)} \sim \text{Im } d_{kn}^i m_{nk}^j, \quad (1)$$

where  $i$  and  $j$  are Cartesian coordinate indices. The tensor  $g_{ij}$  does not vary under time reversal [an  $i$ -tensor (Ref. 2)] and, therefore, does not depend on the properties of the medium regarding the time-reversal operation ( $1'$ ). If the medium is also noninvariant with respect to  $1'$ , it can be characterized by the  $c$ -tensor  $\alpha_{ij}$ , which is odd with respect to both operations, i.e.,  $1'$  and  $\bar{1}$ :

$$\alpha_{ij}^{(nk)} \sim \text{Re } d_{kn}^i m_{nk}^j. \quad (2)$$

The tensor  $\alpha_{ij}$  has the symmetry of the magnetolectric tensor and is, therefore, nonzero in magnetolectric materials. In optics the tensor  $\alpha_{ij}(\omega)$  can produce nonreciprocal effects, such as gyrotropic birefringence for transmitted light and rotation of the polarization plane for reflected light.<sup>3</sup>

Until the recent period experimental investigations of nonreciprocal optical effects have been restricted to studies of the Faraday and Kerr effects in ferro- and ferrimagnets. From the microscopic standpoint these effects are specified by combinations of matrix elements:

$$\text{Im } d_{kn}^i d_{nk}^j \text{ or } \text{Im } m_{kn}^i m_{nk}^j. \quad (3)$$

Terms of type  $dd$  type in (3) make contributions to the antisymmetric part of the dielectric tensor  $\epsilon_{ij}^a(\omega)$ , and terms of type  $mm$  make contributions to the antisymmetric part of the magnetic permeability tensor  $\mu_{ij}^a(\omega)$  (Refs. 4 and 5).

The first theoretical evaluations of the magnitude of the nonreciprocal effects for the antiferromagnet Cr<sub>2</sub>O<sub>3</sub>, which is also magnetolectric and, therefore, has a nonzero magnetolectric tensor  $\alpha_{ij}(\omega)$ , gave very tiny values ( $\sim 10^{-8}$  rad) for the nonreciprocal rotation of the polarization plane for reflected light.<sup>3</sup> In our experiments on the nonreciprocal reflection of light ( $\lambda=0.6328 \mu\text{m}$ ) from Cr<sub>2</sub>O<sub>3</sub> (Ref. 6) we obtained considerably larger values for the rotation of the polarization plane and the ellipticity ( $\approx 10^{-4}$  rad), which agree in order of magnitude with the new microscopic theories.<sup>7-9</sup> An hypothesis that the nonreciprocal effects in Cr<sub>2</sub>O<sub>3</sub> have large values ( $\sim 10^{-3}$ ) was apparently first advanced in Ref. 10.

Since the magnetolectric tensor  $\alpha_{ij}(\omega)$  sensitively depend on the frequency in the region of the  $d-d$  transitions of the Cr<sup>3+</sup> ion, the values of the ellipticity and the rotation of the polarization plane upon reflection observed in Ref. 6 do not provide an adequate picture of the magnitude of the nonreciprocal effects in antiferromagnets, and the agreement with the theoretical evaluations in Refs. 7-9 might be accidental. Therefore, experiments at a fixed wavelength are only the first step in investigating the nonreciprocal effects in antiferromagnets. Undoubtedly, far more complete information on the microscopic mechanisms of such effects in the optical region can be provided by spectroscopic investigations. Their role corresponds as a whole to the role of spectroscopic investigations of the Faraday and Kerr effects in ferro- and ferrimagnets, although there is a significant difference associated with the presence of matrix elements of the magnetic-dipole (or electric-quadrupole) moment in the corresponding susceptibilities.

As far as we know, there have not yet been any reports of spectroscopic investigations of nonreciprocal optical effects in media with a zero macroscopic magnetic moment.

This paper presents the results of spectroscopic investigations of the nonreciprocal optical effects accompanying reflection from Cr<sub>2</sub>O<sub>3</sub>. We shall show that the spectral de-

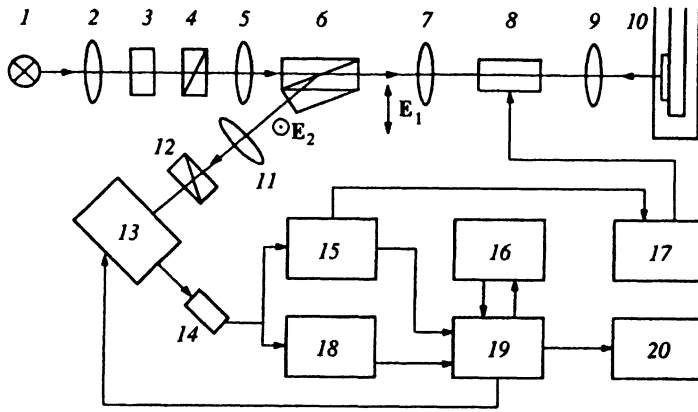


FIG. 1. Diagram of the experimental apparatus.

pendence of the rotation of the polarization plane and the ellipticity of the reflected light contains new information on the electronic transitions and their splitting under the influence of the spin-orbit and exchange interactions.

It is noteworthy that the attempt to interpret the rotation of the polarization plane observed when light is reflected from a GaAs crystal, which does not have magnetic order, as a nonreciprocal effect<sup>11,12</sup> contradicts the invariance of the electromagnetic interactions under time reversal. A critical analysis of this interpretation can be found in Refs. 13 and 14.

## 2. EXPERIMENT

A block diagram of the apparatus used to measure the nonreciprocal rotation of the polarization plane and the nonreciprocal ellipticity of reflected light is presented in Fig. 1. Light from 100-W incandescent lamp 1 passed through water filter 3, polarizer 4 (a Glan prism), and polarization beam splitter 6. Then light with the linear polarization  $E_1$  passed through polarization modulator 8 and was focused by lens 9 onto the sample in cryostat 10. The light reflected from the crystal passed through modulator 8, and the portion of the light with the polarization  $E_2 + E_1$  passing in the opposite direction through the beam splitter 6 was directed onto the inlet slit of monochromator 13. The polarizers 4 and 12, which transmit light with the polarizations  $E_1$  and  $E_2$ , respectively, were used to reduce the level of parasitic light in the optical system. The intensity of the light at the monochromator outlet was measured at the first and second harmonics of the working frequency of the polarization modulator using a photomultiplier and two synchronous detection units, 15 and 18.

For the measurements of the rotation of the polarization plane, a calibrated Faraday cell made from a magneto-optical glass served as the polarization modulator. The amplitude of the modulation of the rotation of the polarization plane was equal to 0.025–0.1 rad in the spectral range 1.5–2.5 eV. The modulation frequency was 400 Hz. The polarization plane was measured by the compensation method. For this purpose an additional constant current was passed through the Faraday cell by automatic compensation unit 17. Its magnitude was such that the constant rotation of the polarization plane in the Faraday cell after two passes would be equal in mag-

nitude and opposite in sign to the rotation resulting from reflection. The sensitivity of the measurements of the rotation of the polarization plane of the reflected light was  $\approx 10^{-5}$  rad.

For the ellipticity measurements, a quartz piezo-optical modulator with a working frequency of 33 kHz served as the polarization modulator 8. The amplitude  $\delta$  of the modulation of the ellipticity was equal to 0.08–0.12 rad in the range from 1.5 to 2.5 eV. The ellipticity  $\varepsilon$  of the reflected light was defined as  $\varepsilon = (\delta/4)I_1I_2$ , where  $I_1$  and  $I_2$  are the amplitudes of the signals at the first and second harmonics of the fundamental frequency of the quartz modulator. The sensitivity of the measurements of the ellipticity of the reflected light was equal to  $\approx 10^{-5}$  rad.

To eliminate any manifestations of the reciprocal optical effects that appear when light passes through the optical elements of the system, the spectral dependence of the rotation of the polarization plane and the ellipticity was measured when the sample was held in two monodomain antiferromagnetic states of the crystal ( $1^+$  and  $1^-$ ) that have opposite spin orientations. The crystals were made monodomain by a magnetoelectric annealing procedure in a constant magnetic field  $H = 2$  kOe and an electric field equal to 100 V/mm. A change in the sign of either of the fields resulted in a change in the sign of the monodomain state of the sample ( $1^+ \leftrightarrow 1^-$ ). After the sample was cooled, the constant fields were removed, and the measurements were performed without external fields, i.e., the spontaneous effects were measured. The difference between the measured values of the rotation of the polarization plane or the ellipticity in the  $1^+$  and  $1^-$  states is determined only by nonreciprocal effects, since the  $1^+$  domain is related to the  $1^-$  domain by the time-reversal operation.<sup>6,15</sup>

The spectral dependence of the rotation of the polarization plane and the ellipticity was measured in the 1.5–2.5 eV range with a resolution equal to 0.002 eV and in the temperature range 40–300 K. The measurements were controlled, and the data were collected and processed using computer 16 and CAMAC interface 19. To monitor the spectral dependence, the intensities of the light at the first and second harmonics were recorded on X–Y potentiometer 20. Averaging of the spectra was employed to increase the sensitivity. The investigations involved the reflection of light from the

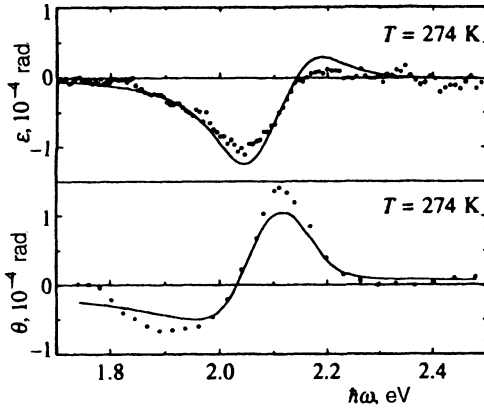


FIG. 2. Nonreciprocal ellipticity and rotation of the polarization plane of linearly polarized light at  $T=274$  K. The solid lines show the results of calculations based on Eq. (4) and the data in Table I.

basal plane of a  $\text{Cr}_2\text{O}_3$  crystal with normal incidence of the light to the surface of the sample. The deviations from normal incidence due to focusing of the light amounted to  $\approx 10^\circ$ .

Below the Néel temperature  $T_N=307$  K a  $\text{Cr}_2\text{O}_3$  crystal belongs to the  $D_{3d}(D_3)$  magnetic point group, which allows a magnetoelectric effect. The  $\text{Cr}_2\text{O}_3$  crystals were cut from boules grown by the Verneuil method. The samples measured  $4 \times 4 \times 0.5$  mm. The surfaces of the crystals were ground and polished by diamond powder. The normal to the sample surface coincided with the  $C_3$  axis to within  $0.2^\circ$ . Silver paste ring electrodes were deposited on the surface of the crystal for applying an electric field. The diameter of the central portion of the crystals not occupied by the electrodes, on which the measurements were performed, was equal to  $\approx 2$  mm.

### 3. RESULTS AND DISCUSSION

Figure 2 presents the spectral dependence of the nonreciprocal ellipticity  $\varepsilon$  and the rotation  $\theta$  of the polarization plane for light reflected from  $\text{Cr}_2\text{O}_3$  at  $T=274$ . Measurements were performed at that temperature only in the 1.8–2.2 eV range, in which the effects observed are governed by the spin-allowed  ${}^4A_2 \rightarrow {}^4T_2$   $d-d$  transition in the  $\text{Cr}^{3+}$  ion.<sup>16</sup> The maximum magnitude of the effects is  $\approx 1 \times 10^{-4}$  rad. We note that the values of the ellipticity and the rotation of the polarization plane at  $\hbar\omega = 1.96$  eV ( $\lambda = 0.63 \mu\text{m}$ ) are consistent with the results of the measurements performed using a polarimetric technique.<sup>6</sup>

Lowering the temperature results in significant variation of the spectral dependence of the rotation of the polarization plane and the ellipticity. At  $T=90$  K (Fig. 3) two broad bands of opposite sign are observed in the spectrum at 1.9–2.3 eV, and narrow intense lines appear at 1.7–1.8 eV. The nonreciprocal rotation of the polarization plane and the ellipticity at 1.9–2.3 eV reach values of  $\approx 2 \times 10^{-4}$  rad, and at 1.7–1.8 eV they amount to  $\approx (7 \pm 1) \times 10^{-4}$  rad.

Figure 4 presents the spectral dependence of the rotation of the polarization plane and the ellipticity at  $T=90$  K in the range from 1.68 to 1.8 eV. As is seen from Fig. 4, the spec-

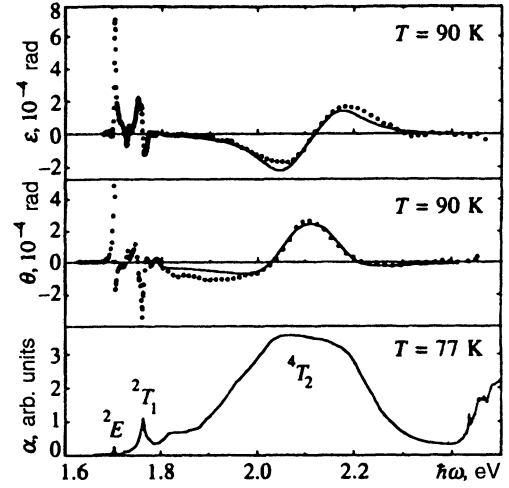


FIG. 3. Nonreciprocal ellipticity and rotation of the polarization plane at  $T=90$  K. The absorption spectrum from Ref. 16 is schematically shown at the bottom.

trum consists of several lines of different intensity and different sign. The positions of the lines correlate with the lines observed in the absorption spectrum of  $\text{Cr}_2\text{O}_3$  (Ref. 16). The spectra of the ellipticity  $\varepsilon(\omega)$  and the rotation  $\theta(\omega)$  are approximated well by a sum of Lorentzian functions:

$$\theta + i\varepsilon = \sum_n \frac{A_n}{\omega_n^2 - \omega^2 - i\omega\Gamma_n}, \quad (4)$$

where  $\omega_n$  is the transition frequency,  $\gamma_n$  is the damping, and  $A_n$  is the amplitude. The values of  $\omega_n$ ,  $\Gamma_n$ , and  $A_n$  obtained from the conditions of best fit with the experiment are presented in Table I, and the corresponding plots of  $\varepsilon(\omega)$  and  $\theta(\omega)$  are depicted in Figs. 2–4 by solid lines.

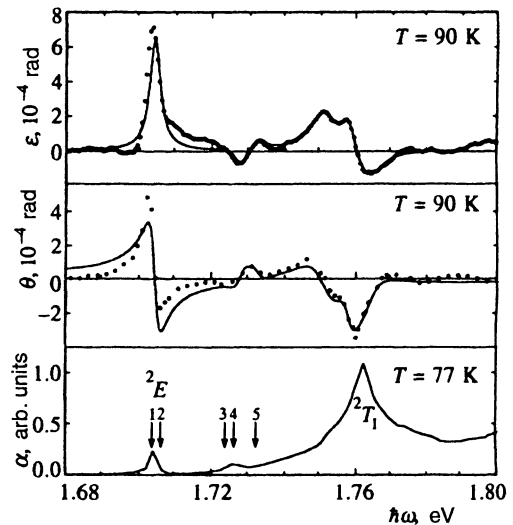


FIG. 4. Nonreciprocal ellipticity and rotation of the polarization plane at  $T=90$  K in the region of the spin-forbidden  ${}^4A_2 \rightarrow {}^2E$  and  ${}^4A_2 \rightarrow {}^2T_1$  transitions.

TABLE I. Parameters  $\omega_n$ ,  $A_n$ , and  $\Gamma_n$  in Eq. (4).

Transition	$\omega_n$ , eV	$A_n$ , (eV) <sup>2</sup>	$\Gamma_n$ , eV
${}^4A_2 - {}^2E$	1.704	$3.9 \times 10^{-2}$	$3.5 \times 10^{-3}$
	1.727	$-5.6 \times 10^{-3}$	$3.5 \times 10^{-3}$
	1.732	$4.6 \times 10^{-3}$	$4.2 \times 10^{-3}$
${}^4A_2 - {}^2T_1$	1.751	$4.0 \times 10^{-2}$	$10^{-2}$
	1.758	$1.4 \times 10^{-3}$	$4.4 \times 10^{-3}$
	1.763	$-3.3 \times 10^{-2}$	$9.6 \times 10^{-3}$
${}^4A_2 - {}^4T_2$	2.051	-0.8	0.14
	2.169	0.62	0.14

The ellipticity  $\varepsilon$  and the rotation  $\theta$  observed when light is reflected from  $\text{Cr}_2\text{O}_3$  are related in the geometry under consideration to components of the magnetoelectric tensor by the expression<sup>3</sup>

$$\theta + i\varepsilon = 2\alpha_{\perp}(1 + n_{\perp})/(1 - n_{\perp}), \quad (5)$$

where  $\alpha_{\perp} = \alpha_{xx}(\omega) = \alpha_{yy}(\omega)$  is a component of the magnetoelectric tensor and  $n_{\perp}^2 = \varepsilon_{xx}(\omega) = \varepsilon_{yy}(\omega)$ . Because of the weakness of the  $d-d$  transitions, the dispersion of  $n_{\perp}(\omega)$  in the frequency range considered is small, and, as can be seen from (5), the spectral dependence of  $\theta$  and  $\varepsilon$  is determined mainly by that of  $\text{Re } \alpha_{\perp}(\omega)$  and  $\text{Im } \alpha_{\perp}(\omega)$ . If the excitonic effects are neglected, the tensor  $\alpha_{ii}(\omega)$  can be represented in the region of the  $d-d$  transitions as the sum of the contributions  $\alpha_{ii}^{\text{ion}}(\omega)$  of the  $\text{Cr}^{3+}$  ions:<sup>1,3</sup>

$$\alpha_{ii}^{\text{ion}}(\omega) = \frac{4\pi}{\hbar} \sum_{k,n} \rho_k \left( \frac{\text{Re } d_{nk}^i m_{kn}^i}{\omega_{nk} + \omega + i\Gamma_{nk}} + \frac{\text{Re } m_{kn}^i d_{nk}^i}{\omega_{nk} - \omega - i\Gamma_{nk}} \right), \quad (6)$$

where  $n$  and  $k$  are states of the  $\text{Cr}^{3+}$  ion,  $\hbar\omega_{nk} = E_n - E_k$  is the energy of the transition between states  $n$  and  $k$ ,  $\Gamma_{nk}$  is the damping, and  $\rho_k$  is the probability of finding the ion in state  $k$ . The parameters of the Lorentzian functions (4) and the magnetoelectric susceptibility (6) are related by the expressions

$$A_n = 2\omega_{nk} \text{Re } d_{kn}^i m_{nk}^j, \quad \omega_n^2 = \omega_{nk}^2 + \Gamma_{nk}^2, \quad \Gamma_n = 2\Gamma_{nk}.$$

The tensor  $\alpha_{ij}$  vanishes above the Néel temperature due to the space-inversion and time-reversal symmetry of the crystal. Below  $T_N$  the magnetic symmetry of  $\text{Cr}_2\text{O}_3$  is such that each  $\text{Cr}^{3+}$  ion makes the same contribution  $\alpha_{ii}^{\text{ion}}(\omega)$  to the magnetoelectric tensor,<sup>3</sup> i.e.,  $\alpha_{ii}(\omega) = \mathcal{N}\alpha_{ii}^{\text{ion}}(\omega)$ , where  $\mathcal{N} = 4 \times 10^{22} \text{ cm}^{-3}$  is the density of the  $\text{Cr}^{3+}$  ions.

In the optical frequency range the magnetoelectric  $c$ -tensor  $\alpha_{ij}(\omega)$  appears as a component part of the third-rank  $c$ -tensor  $\gamma_{ikl}^s(\omega)$ , which is symmetric under transposition of the indices  $i$  and  $k$  and describes the spatial dispersion of the dielectric tensor that is linear with respect to the wave vector  $\mathbf{k}$  (Ref. 3):

$$\epsilon_{ik}(\omega, \mathbf{k}) = \epsilon_{ik}(\omega) + \gamma_{ikl}^s k_l.$$

When the tensor  $\gamma_{ikl}^s$  is expanded in representations of the rotation group, the part of this expansion which transforms as a second-rank tensor with a trace equal to zero is the magnetoelectric tensor. The other part of this expansion, which transforms as a third-rank tensor  $s_{ikl}$  that is symmetric

toward permutations of all the indices, is associated with the electric-quadrupole moments of the ions and does not make a contribution to the nonreciprocal effects observed when light is reflected in the geometry under consideration.<sup>6</sup> We note that the tensor  $s_{ikl}$  can be nonzero in antiferromagnets that are not magnetoelectric.

As was pointed out above, the tensor  $\gamma_{ikl}^s$  nonuniquely specifies the diagonal components  $\alpha_{ii}$  of the magnetoelectric tensor. This means that the diagonal components of the magnetoelectric tensor cannot be determined from measurements of bulk effects alone, i.e., effects observed when light propagates in a homogeneous medium. The diagonal components of the magnetoelectric tensor are related to the dielectric tensor of an inhomogeneous medium<sup>6</sup> and, therefore, can be measured in reflection experiments. In this connection we note that the expression (6) for the magnetoelectric tensor is approximate and corresponds to the neglect of all effects associated with the presence of a surface. These effects can be divided into two groups according to their physical origin. The first group includes the surface effects caused by the distortion of the electronic states near the surface. Such effects should not play a significant role in the frequency range of the intra-ionic  $d-d$  transitions. The other group of surface effects is associated with the discrete nature of the crystal lattice. Nonreciprocal effects of this type can be observed only in cases in which the crystal surface is nearly ideal,<sup>8</sup> but such a case is certainly not observed in the sample that we used. In addition, an evaluation of the Faraday effect in  $\text{Cr}_2\text{O}_3$  in the frequency range investigated from one layer of  $\text{Cr}^{3+}$  ions having spins of identical orientation using the results in Ref. 17 gives a value of the nonreciprocal effects in reflection equal to  $\sim 10^{-6} - 10^{-7}$ , which is several orders of magnitude below the values observed. Thus, the use of (6) to analyze nonreciprocal rotation and ellipticity spectra is physically justified.

The optical absorption in  $\text{Cr}_2\text{O}_3$  (Ref. 16) is characterized by two broad bands, which are caused by transitions from the ground state  ${}^4A_2$  of the  $\text{Cr}^{3+}$  ion to the excited states  ${}^4T_2$  and  ${}^4T_1$ . In addition, there are several narrow lines associated with spin-forbidden transitions to the  ${}^2E$ ,  ${}^2T_1$ , and  ${}^2T_2$  states. The  $\text{Cr}^{3+}$  ions are found in trigonally distorted octahedrons with  $C_3$  site symmetry, and, therefore, the cubic terms are actually a set of levels located in the energy range  $\Delta E < v \approx 0.1$  eV, where  $v$  is the characteristic energy of the trigonal field.

Let us consider the spin-allowed  ${}^4A_1 \rightarrow {}^4T_2$  transition. As is seen from Fig. 3 and the data in Table I, this transition is split into two bands at 2.051 and 2.169 eV. It can be postulated that these bands correspond to transitions to levels belonging to the trigonal terms  ${}^4A'$  and  ${}^4E'$ , which appear as a result of trigonal splitting of the cubic term  ${}^4T_2$ . Such an explanation must be justified for the following reasons. First, it is generally known<sup>18</sup> that trigonal splitting cannot be observed in absorption in an axial geometry, i.e., when the wave vector  $\mathbf{k}$  is parallel to the  $C_3$  axis. Second, the magnitude of the observed splitting ( $\approx 0.12$  eV) is appreciably greater than the magnitude of the trigonal splitting observed when  $\mathbf{k}$  is perpendicular to the  $C_3$  axis in absorption experiments,<sup>16</sup> which was found to depend both on the tem-

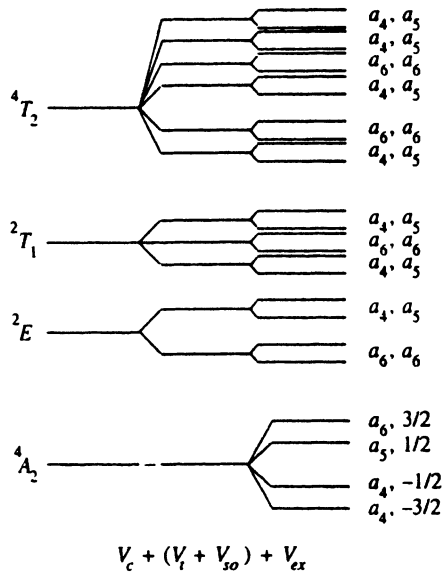


FIG. 5. Splitting scheme of the terms of the  $\text{Cr}^{3+}$  ion in cubic ( $V_c$ ) and trigonal ( $V_i$ ) crystal fields with consideration of the spin-orbit ( $V_{so}$ ) and exchange ( $V_{ex}$ ) interactions.

perature and on the sample and to fall in the range between 0.04 and 0.09 eV.

To explain the origin of the bands at 2.051 and 2.169 eV, let us consider the structure of the energy levels arising from the cubic terms  ${}^4A_2$  and  ${}^4T_2$  under the action of trigonal and exchange fields, as well as the spin-orbit interaction, in greater detail (Fig. 5). We use the notation  $a_1$ – $a_6$  for the representations of the double trigonal  $C_3$  group, whose characters  $\chi(C_3)$  are equal to 1,  $e^{2\pi i/3}$ ,  $e^{-2\pi i/3}$ ,  $e^{\pi i/3}$ ,  $e^{-\pi i/3}$ , and  $-1$ , respectively. When  $\alpha_{\perp}$  is evaluated using Eq. (6), only the contributions that are linear with respect to the spin-orbit interaction should be taken into account. This follows from a general symmetry treatment of the magnetoelectric effect in antiferromagnets (see, for example, Ref. 19), according to which the component  $\alpha_{\perp}$  for collinear ordering of the spins is nonzero only when the spin-orbit interaction is taken into account. This can be seen using Eq. (6), if we note that only the matrix elements which are diagonal with respect to the spin quantum indices can appear in (6) in the exchange approximation (since  $\mathbf{d}$  is the orbital operator). In this case  $(\mathbf{m}_{\perp})_{nk} \sim \langle \mathbf{S}_{\perp} \rangle = 0$ .

In the linear approximation the spin-orbit interaction does not mix the components of the ground-state multiplet  $|{}^4A_2, M_S\rangle$  of the  $\text{Cr}^{3+}$  with one another. Therefore, we can select the  $|{}^4A_2 - 3/2\rangle$  state, which transforms in the  $C_3$  group according to the  $a_6$  representation, as the ground state of the  $\text{Cr}^{3+}$  ion. For  $T < 100$  K the populating of all the components of the ground-state multiplet, except the lowest, can be neglected with good accuracy.

A trigonal field splits the cubic term  ${}^4T_2$  into two terms of the  $C_3$  group, viz.,  ${}^4A'$  and  ${}^4E'$  with the wave functions  $|a, M_S\rangle$  and  $|u_{\pm}, M_S\rangle$ , respectively, where  $M_S = \pm 3/2, \pm 1/2$ , and the spin-orbit interaction mixes these states, so that the pairs of Kramers doublets  $(a_4, a_5)$  and  $(a_6\uparrow, a_6\downarrow)$  form as a result. Here the arrows denote different functions

that transform according to the same irreducible representation  $a_6$ . The exchange field removes the Kramers degeneracy, so that the  ${}^4T_2$  term splits into 12 nondegenerate states as a result (see Fig. 5). We note that the exchange field does not lower the  $C_3$  site symmetry. An analysis of the splitting is greatly facilitated, if it is taken into account that the pairs of states  $|u_{\pm}, \pm 3/2\rangle$ ,  $|u_{\pm}, \mp 3/2\rangle$ ,  $|u_{\mp}, \pm 1/2\rangle$ , and  $|a, \mp 1/2\rangle$  transform as the Kramers doublets, and the pairs of states  $|u_{\pm}, \pm 1/2\rangle$  and  $|a, \mp 1/2\rangle$  transform as  $(a_6\uparrow, a_6\downarrow)$ .

The selection rules for the matrix elements of the operators, which are identical for the moments  $\mathbf{d}$  and  $\mathbf{m}$  in the  $C_3$  group, allow transitions from the  $a_6$  ground state to states with  $a_4$  and  $a_5$  symmetries in the longitudinal geometry. Taking into account the selection rules with respect to the spin projection, we can show that the transitions to the  $\Psi_1$  and  $\Psi_2$  states with  $a_4$  symmetry are allowed:

$$\Psi_1 = \left| u_+ - \frac{3}{2} \right\rangle + \beta \left| a - \frac{1}{2} \right\rangle \quad (7)$$

$$\Psi_2 = \left| a - \frac{1}{2} \right\rangle - \beta^* \left| u_+ - \frac{3}{2} \right\rangle.$$

Here  $\beta \sim \lambda_{so}/v$ , where  $\lambda_{so}$  is the spin-orbit coupling constant and  $v$  is the magnitude of the trigonal splitting. We note that the splitting scheme of the  ${}^4T_2$  term in Fig. 5 corresponds to the condition  $v < 0$  (Ref. 16); however, the relative position of the Kramers doublets is shown arbitrarily. Using Eq. (6), we can show that the transitions to the states (7) make contributions to  $\alpha_{\perp}(\omega)$  that are equal in absolute value, but opposite in sign. Hence it follows that the ellipticity  $\varepsilon(\omega)$  should have two peaks in the region of the  ${}^4A_2 \rightarrow {}^4T_2$  transition that are equal in absolute amplitude and opposite in sign, which correspond to transitions to the trigonal terms  ${}^4E'$  and  ${}^4A'$ . Qualitatively similar behavior of the ellipticity was observed experimentally (see Fig. 3). Of course, the expressions (7) for the wave functions are approximate, since they do not take into account the admixtures of other cubic terms, primarily of the spin-orbit mixing of the ground state  $|{}^4A_2 - 3/2\rangle$  with components of the  ${}^4T_2$  multiplet. The degree of this mixing is specified by the parameter  $\lambda_{so}/K$ , where  $K$  is the characteristic energy of the cubic component of the crystal field. Since  $K \gg v$  holds, the contribution of such states to  $\alpha_{\perp}$  is  $v/K$  times smaller than the contribution of the states (7) and only slightly distorts the simple picture of two peaks of equal amplitude and opposite sign.

The proposed model qualitatively accounts for the difference between the magnitudes of the trigonal splittings in the present work and in Ref. 16. The difference ( $\approx 0.05$  eV) appears because the largest contribution to the absorption and to the nonreciprocal reflection of light is made by transitions to different levels of the split  ${}^4T_2$  cubic term. In the absorption experiments<sup>16</sup> the trigonal splitting is determined by comparing the  $\sigma$  and  $\pi$  spectra, and the latter spectrum is formed mainly as a result of transitions to the  $a_6$  level ( ${}^4A'$ ). Since the exchange and spin-orbit splitting in  $\text{Cr}_2\text{O}_3$  fall in the range from 0.01 to 0.03 eV (Refs. 16, 18, and 20), the values of  $\approx 0.05$  eV can be fully attributed to the combined effect of the exchange and spin-orbit interactions on the  ${}^4T_2$  term. More exact quantitative evaluations are made

difficult by a lack of exact information on the values of the constants characterizing the interactions in the  $\text{Cr}^{3+}$  ion.

Let us now consider the spin-forbidden  ${}^4A_2 \rightarrow {}^2E$  transition, which corresponds to the  $R_1$  and  $R_2$  lines in the ruby  $\text{Al}_2\text{O}_3:\text{Cr}^{3+}$ . It was established in Ref. 20–24 that at low temperatures the spectrum of  $\text{Cr}_2\text{O}_3$  contains five narrow lines 1–5 in the region of the single-ion  ${}^4A_2 \rightarrow {}^2E$  transition with energies equal to 1.7036, 1.7062, 1.7234, 1.7263, and 1.7322 eV, respectively. There is presently no doubt that these lines are associated with excitonic excitations, but partially different identifications of the lines were given in different papers.<sup>22,24</sup>

The wave functions of the excitons in the magnetically ordered state of  $\text{Cr}_2\text{O}_3$  transform according to the irreducible representation of the unitary  $D_3$  subgroup of the magnetic  $D_{3d}$  group. A symmetry analysis shows<sup>24</sup> that the Davydov splitting of the transitions from the lowest spin level of the ground-state  ${}^4A_2$  multiplet to the lowest spin levels of the  ${}^2E$  multiplet results in the appearance of two  $E$  excitons and two  $A_2$  excitons. In the longitudinal geometry the selection rules in the  $D_3$  group allow excitation of only  $E$  excitons. This applies both to the absorption experiments and to our experiment, since the vectors  $\mathbf{d}$  and  $\mathbf{m}$  transform in  $D_3$  according to the same reducible representation  $A_2 + E$ .

Here it is important to stress that Eq. (6) for  $\alpha_{\perp}(\omega)$  can be used to analyze the excitonic part of the spectrum, if  $n$  and  $k$  are understood to be excitonic excitations. This is because the center zone  $\mathbf{k}=0$  of the Brillouin is an extremum of the exciton energy  $\mathcal{E}(\mathbf{k})$  in  $\text{Cr}_2\text{O}_3$  (Ref. 23), and, therefore, the excitonic dispersion does not make a contribution to the magnetoelectric tensor.<sup>3</sup> Another factor which greatly simplifies the analysis of the excitonic contribution is the absence of new values at the excitonic resonance  $\hbar\omega = \mathcal{E}(\mathbf{k})$  when light propagates along the  $C_3$  axis, and there is consequently no need in this case to impose additional boundary conditions to calculate the reflection of light.<sup>25</sup> Therefore, Eq. (5), which was obtained using only Maxwellian boundary conditions, is also applicable in the region of excitonic resonance.

As is seen from Fig. 4, three lines are observed in the region of the  ${}^4A_2 \rightarrow {}^2E$  transition at energies corresponding to lines 1, 4, and 5 that were observed in Ref. 20–22. In Ref. 22 lines 1 and 4 were interpreted as  $E$  excitons, and line 5 was interpreted as an exciton-magnon excitation.<sup>22</sup> The fact that line 5 was observed in our experiment points out the  $E$  symmetry of this excitation and is not consistent with the hypothesis in Ref. 24 that line 5 is a manifestation of an  $A_2$  exciton. At the same time, our data are not completely consistent with the data and interpretation in Ref. 22. In Ref. 22 five lines were observed when the wave vector  $\mathbf{k}$  was perpendicular to the  $C_3$  axis in  $\sigma$  and  $\pi$  polarization, but were not observed in the longitudinal geometry, i.e., in the geometry of our experiment. In addition, the exciton theory devised for the case under consideration in Ref. 22 gives ellipticities of the same sign for both  $E$  excitons (lines 1 and 4), while we observed ellipticities of different sign. We note that lines 1, 4, and 5 were also observed in experiments on generating the second optical harmonic in  $\text{Cr}_2\text{O}_3$ , but with significantly different relative intensities.<sup>26</sup> In the spectrum

of the second harmonic line 1 is several orders of magnitude more intense than lines 4 and 5.

The other spin-allowed transition in the  $\text{Cr}^{3+}$  ion,  ${}^4A_2 \rightarrow {}^2T_1$ , was thoroughly investigated in ruby and scarcely studied in  $\text{Cr}_2\text{O}_3$ . Comparing the position of the absorption lines with our spectra, we naturally assume that the group of three lines (1.751, 1.758, and 1.763 eV) corresponds to the  ${}^4A_2 \rightarrow {}^2T_1$  transition. The cubic term  ${}^2T_1$  is split by the trigonal crystal field and the spin-orbit interaction into three Kramers doublets (see Fig. 5). To remove the spin prohibition, the admixture of  ${}^4T_2$  states must be taken into account. Using the results of the theoretical analysis of the absorption spectrum of the  $\text{Cr}^{3+}$  ion in ruby,<sup>17</sup> we can show that the main contribution to  $\alpha_{\perp}(\omega)$  in the  ${}^2T_1$  region is made by transitions to levels with  $a_4$  and  $a_5$  symmetries that belong to different Kramers doublets:  $|a_4\rangle \approx |a_0 - 1/2\rangle$ ,  $a_5 \approx |a_+ - 1/2\rangle$ . Here  $a_0$  and  $a_{\pm}$  are the trigonal components of the  $T_1$  term.<sup>18</sup> If this simple picture were correct, we should have observed two lines separated by an energy gap of  $\sim 0.01$  eV in the region of the  ${}^2T_1$  transition. However, we observed three clearly expressed lines (see Fig. 4), whose appearance cannot be explained by such a simple model. A more rigorous treatment leads to a picture of energy levels that depends on the relationship between the trigonal field, the exchange interaction, and the spin-orbit interaction; however, positions of the levels that are qualitatively similar to the experimentally observed positions could not be obtained for any values of the parameters. It can, therefore, be postulated that excitonic effects must be taken into account in the analysis of the splitting of the  ${}^2T_1$  term in the magnetically ordered state of  $\text{Cr}_2\text{O}_3$ , as was done in the treatment of the  ${}^4A_2 \rightarrow {}^2E$  transition. To avoid any misunderstandings, we note that in ruby the  ${}^4A_2 \rightarrow {}^2T_1$  transition is also split into three lines, but this is associated with equal populating of all the spin components of the ground-state multiplet in the absence of magnetic ordering.

We have already pointed out several significant differences between the data obtained from absorption experiments and measurements of nonreciprocal optical effects. We note one more difference here. Since the product of matrix elements  $d_{kn}m_{nk}$  is proportional to the odd part of the trigonal field  $v_o$ ,  $\alpha_{\perp}(\omega) \sim \lambda_{so}v_o$  holds for the spin-allowed  $d-d$  transitions (see also Ref. 7), while  $\alpha_{\perp}(\omega) \sim \lambda_{so}^2v_o$  holds for the spin-forbidden  $d-d$  transitions. The ratio between these quantities is proportional to  $\lambda_{so}$ , while the ratio between the intensities of these transitions in absorption is proportional to  $\lambda_{so}^2$  (Ref. 18).

#### 4. CONCLUSIONS

In this work we have investigated the electronic spectrum of antiferromagnets for the first time using a new type of spectroscopy, which can be applied to all materials with macroscopically broken time-reversal and space-inversion symmetry. The spontaneous nonreciprocal rotation of the polarization plane and circular dichroism observed when linearly polarized light is reflected from  $\text{Cr}_2\text{O}_3$  have been investigated. The experimental manifestations of these phenomena are similar to those of the familiar polar Kerr

effect in ferro- and ferrimagnets. However, unlike the Kerr effect, which is governed by the magnetic moment, these effects are observed in the magnetically ordered state of  $\text{Cr}_2\text{O}_3$  in the absence of a magnetic moment. We have shown that the spectral dependence obtained in our experiments can be interpreted when the trigonal and exchange fields, as well as the spin-orbit interaction, are simultaneously taken into account. An analysis of the spectra of the nonreciprocal effects in the region of the spin-forbidden transitions has confirmed the formation of magnetic excitons, although the data that we obtained are not completely consistent with any of the previously proposed interpretations of the absorption spectra in this energy range. Finally, we note that there is a possibility, in principle, of using spectroscopic measurements of nonreciprocal optical effects to investigate not only magnetoelectric materials, but also any antiferromagnets in which the time-reversal symmetry breaking has a macroscopic character, for example, piezomagnetic crystals. From the standpoint of phenomenological electrodynamics, such effects appear as a result of spatial dispersion of the dielectric tensor  $\epsilon_{ik}(\omega, \mathbf{k})$ , and, generally speaking, they are characterized by smaller values than are the nonreciprocal effects in ferromagnets. Nevertheless, as the present work shows, experimental investigations of these materials are fully possible.

This work was supported by the Russian Fund for Fundamental Research and the International Science Foundation.

<sup>1</sup>L. D. Baron, *Molecular Light Scattering and Optical Activity*, Cambridge University Press, Cambridge (1982).

<sup>2</sup>R. R. Birss, *Symmetry and Magnetism*, North-Holland, Amsterdam (1966).

<sup>3</sup>R. M. Hornreich and S. Shtrikman, *Phys. Rev.* **171**, 1065 (1968).

- <sup>4</sup>G. S. Krinchik and M. V. Chetkin, *Zh. Éksp. Teor. Fiz.* **36**, 1924 (1959) [*Sov. Phys. JETP* **9**, 1368 (1959)].
- <sup>5</sup>G. S. Krinchik and M. V. Chetkin, *Zh. Éksp. Teor. Fiz.* **41**, 673 (1961) [*Sov. Phys. JETP* **14**, 485 (1962)].
- <sup>6</sup>B. B. Krichevstov, V. V. Pavlov, R. V. Pisarev, and V. N. Gridnev, *J. Phys.: Condens. Matter* **5**, 8233 (1993).
- <sup>7</sup>V. N. Muthukumar, R. Valenti, and C. Gros, *Phys. Rev. Lett.* **75**, 2766 (1995).
- <sup>8</sup>I. Dzyaloshinskii and E. V. Papamichail, *Phys. Rev. Lett.* **75**, 3004 (1995).
- <sup>9</sup>E. B. Graham and R. E. Raab, *Philos. Mag.* **66**, 269 (1992).
- <sup>10</sup>V. M. Agranovich and V. L. Ginzburg, in *Progress in Optics*, E. Wolf (ed.), North-Holland, Amsterdam (1971), Vol. 9, p. 237.
- <sup>11</sup>N. I. Zheludev, S. V. Popov, Y. P. Svirko *et al.*, *Phys. Rev. B* **50**, 11 508 (1994).
- <sup>12</sup>N. I. Zheludev, S. V. Popov, Y. P. Svirko *et al.*, *Phys. Rev. B* **52**, 2203 (1995).
- <sup>13</sup>L. C. Lew Yan Voon, A. Fainstein, P. Etchegoin *et al.*, *Phys. Rev. B* **52**, 2201 (1995).
- <sup>14</sup>E. L. Ivchenko, *Fiz. Tverd. Tela (St. Petersburg)* **38**, 2066 (1996) [*Phys. Solid State* **38**, 1140 (1996)].
- <sup>15</sup>A. L. Shelankov and G. E. Pikus, *Phys. Rev. B* **46**, 3326 (1992).
- <sup>16</sup>D. S. McClure, *J. Chem. Phys.* **38**, 2289 (1963).
- <sup>17</sup>B. B. Krichevstov, V. V. Pavlov, and R. V. Pisarev, *Zh. Éksp. Teor. Fiz.* **94**, 284 (1988) [*Sov. Phys. JETP* **67**, 378 (1988)].
- <sup>18</sup>S. Sugano and Y. Tanabe, *J. Phys. Soc. Jpn.* **13**, 880 (1958).
- <sup>19</sup>I. M. Vitebskii, N. M. Lavrinenko, and V. L. Sobolev, *J. Magn. Magn. Mater.* **97**, 263 (1991).
- <sup>20</sup>K. A. Wickersheim, *J. Appl. Phys.* **34**, 1224 (1963).
- <sup>21</sup>J. P. van der Ziel, *Phys. Rev. Lett.* **18**, 237 (1967).
- <sup>22</sup>J. W. Allen, R. M. Macfarlane, and R. L. White, *Phys. Rev.* **179**, 523 (1969).
- <sup>23</sup>R. M. Macfarlane and J. W. Allen, *Phys. Rev. B* **4**, 3054 (1971).
- <sup>24</sup>J. W. Allen, *Phys. Rev. B* **9**, 259 (1974).
- <sup>25</sup>V. M. Agranovich and V. L. Ginzburg, *Crystal Optics with Spatial Dispersion, and Excitons*, 2nd ed., Springer-Verlag, Berlin-New York (1984).
- <sup>26</sup>M. Fiebig, D. Fröhlich, B. B. Krichevstov, and R. V. Pisarev, *Phys. Rev. Lett.* **73**, 2127 (1994).

Translated by P. Shelnitz